PERGAMON

International Journal of Heat and Mass Transfer 43 (2000) 3835–3846

International Journal of HEAT and MASS TRANSFER

www.elsevier.com/locate/ijhmt

Thermal modeling of selective area laser deposition of titanium nitride on a finite slab with stationary and moving laser beams

Yuwen Zhang, A. Faghri*

Department of Mechanical Engineering, University of Connecticut, 191 Auditorium Road, Storrs, CT 06269-3139, USA

Received 26 January 1999; received in revised form 10 December 1999

Abstract

A thermal model of selective area laser deposition of titanium nitride on a finite slab under irradiation by a stationary or a moving laser beam is presented in this paper. Heat transfer in the substrate and gases, the chemical reaction on the substrate's top surface, and the mass transfer of gases in the chamber were taken into account in the model. For the cases of the stationary laser beam, the predicted deposited film profile was in good agreement with the experimental results. For the cases of the moving laser beam, the deposited film became higher and wider when the scanning velocity was decreased or the laser power was increased. Because of the low sticking coefficient of TiN at high temperature, a groove appeared on the top of the deposited film when high laser power was applied. © 2000 Elsevier Science Ltd. All rights reserved.

1. Introduction

Solid Freeform Fabrication (SFF) with Selective Area Laser Deposition (SALD) is a emerging manufacturing technology that directly creates three dimensional parts from a CAD design [1]. SALD utilizes Laser Chemical Vapor Deposition (LCVD) technique, which can be based on reactions initiated pyrolytically, photolytically or a combination of both [2], to deposit the film at the desired location on the substrate. Pyrolytic LCVD uses a laser beam, which is not absorbed by the gaseous material, to locally heat the substrate to produce a hot spot where a thermally assisted chemical reaction takes place. The product of the chemical reaction, which is a film of material, sticks to the substrate surface due to chemisorption. On the other hand, photolytic LCVD involves tuning the laser to an electric or vibrational level of the gas. The irradiated material decomposes and the products deposit on the cooler substrate to form the film.

Chemical Vapor Deposition (CVD) has been extensively investigated by many researchers and a detailed literature review is given by Mahajan [3]. In a pyrolytic CVD process, the entire substrate is heated, and vapor deposition occurs throughout the entire substrate. On the other hand, in the SALD process, only a very small spot on the substrate is heated by the laser beam and vapor deposition occurs only in the heated spot. A very detailed literature review about Laser Chemical Vapor Deposition (LCVD) is given by Mazumder and Kar [4]. Kar and Mazumder [5] present a 3D transient thermal analysis for laser chemical vapor deposition on a uniformly moving slab, in which a 3D, non-lin-

* Corresponding author. Tel.: +1-860-486-2221; fax: +1-860-486-0318.

E-mail address: faghri@eng2.uconn.edu (A. Faghri).

0017-9310/00/$ - see front matter © 2000 Elsevier Science Ltd. All rights reserved.
PII: S0017-9310(99)00396-8

Nomenclature

C	concentration (kg/m^3)
c_p	specific heat (J/kg K)
D	mass diffussivity (m^2/s)
E	activation energy (kJ/mol)
H	height of the chamber (m)
h	thickness of the substrate (m)
k	thermal conductivity (W/mK)
K_0'	Arrhenius constant
K_0	$(C_{H_2})_i\,(C_{N2})_i^{1/2}K_0'$ (m/s)
L	length of the chamber (m)
l	length of the substrate (m)
M	molecular weight (g/mol)
$\dot{m}$	mass flux (kg/m^2)
P	laser power (W)
q''	heat flux (W/m^2)
r_0	radius of the laser beam (m)
R_u	universal gas constant ($=8.314$ kJ/kmol)
S	source term in the energy equation
S_c	source term in the mass transfer equation
t	time (s)
T	temperature (K)
u	laser scanning velocity (m/s)
W	width of the chamber (m)
w	width of the substrate (m)
x	coordinate in longth direction (m)
y	coordinate in width direction (m)
z	coordinate height direction (m)

Greek symbols

α_a	absorptivity
γ	sticking coefficient
δ	thickness of the deposited film (m)
ΔH_R	heat of chemical reaction (J/kg)
ε	emissivity
ρ	density (kg/m^3)

Subscripts

g	gas
i	initial value
s	substrate
st	start point
∞	infinite

ear, transient conduction problem is solved analytically. The heat conduction equation is then linearized by introducing Kirchoff's transformation to account for the variable thermal properties, and the boundary condition is linearized by introducing an effective convective heat transfer coefficient. The linearized heat conduction equation is solved by a Fourier transformation method. Kar et al. [6] investigate laser chemical vapor deposition of titanium on stationary finite slabs by solving 3D, transient mass diffusion equations for each species using Fourier's transformation method. Conde et al. [7] present a thermal model of laser chemical vapor deposition of TiN dots produced by the following overall chemical reaction on the substrate surface:

$$TiCl_4(g) + 2H_2(g) + \frac{1}{2}N_2(g) \rightarrow TiN(s) + 4HCl(g) \qquad (1)$$

The 3D transient diffusive mass transfer equation is solved using Fourier's transformation method. The volcano-like profile of the deposited film is found in certain conditions, which was in good agreement with the experimental data [8]. The authors of Refs. [6,7] do not consider the heat transfer of the gases in the chamber. Another assumption in Refs. [5–7] is that the effect of chemical reaction heat on the heat conduction of the substrate is negligible. This assumption can significantly simplify the analytical/numerical procedure because heat conduction in the substrate is not coupled with heat/mass transfer in the gas and the chemical reaction under this assumption.

Marcus et al. [2] study the residual stresses in laser processed SFF, which includes SALD. Heat conduction in the substrate is modeled as a pure conduction problem with a moving heat source. Jacquot et al. [9] propose a thermal model of the SALD process using acetylene as the source gas. Various phenomena, which include heat conduction in the substrate, chemical reaction during carbon deposit, and mass diffusion of acetylene in the chamber are taken into account. The effect of chemical reaction heat on the heat conduction of the substrate is taken into account. The temperature of the gases is assumed to be uniform and, therefore, the heat transfer in the gas phase is neglected.

The effect of natural convection of the gases is neglected by many researchers [6,7,9] except Lee et al. [10] who numerically predict the deposit rate using pure tetramethylsilane [$Si(CH_3)_4$] as a precursor for a rod grown by the SALD process. However, their results indicate that the heat and mass transfer in the gases are dominated by diffusion, and the effect of natural convection of the gas is negligible. In reality, the effect of natural convection is important only if the total pressure in the chamber is high. However, the total pressure of the gases in the chamber of the SALD process is on the order of 10^2 torr [7,8,10], and therefore it is

expected that the effect of natural convection on the vapor deposition is insignificant. An estimation of Grashof numbers for different cases investigated in Refs. [7,10] indicated that the their order of magnitude for different cases are in the order of 1 or less [11]. Since natural convection can play a significant role only if the Grashof number is on or greater than the order of magnitude to 10^3 [12], the effect of natural convection in the SALD process can be safely neglected.

The SALD process is very complicated because it involves heat transfer in the substrate, heat and mass transfer in the gases, and a chemical reaction on the substrate surface under the laser spot. It appears that none of the existing thermal models deal with the above complicated coupled phenomena. In this paper, a thermal model of SALD process will be developed to predict the shape of deposited film. The SALD process with both stationary and moving laser beam will be investigated. The numerical results will be compared with the experimental data in the existing literature. The effect of laser power and scanning velocity on the SALD process will also be investigated.

2. Physical model

The physical model of SALD is shown in Fig. 1. A substrate made of Incoloy 800 with a size of $2l \times 2w \times h$ (length × width × height) is located in the center of the bottom surface of a chamber with a size of $2L \times 2W \times H$ (length × width × height). Before the vapor deposition started, the chamber was evacuated then filled with mixture of H_2, N_2, and $TiCl_4$. For the cases of stationary laser beam, the center of the laser beam is located at the center of the top surface of the substrate ($x = 0$, $y = 0$, $z = h$). For the cases of the moving laser beam, the laser beam scans the surface of the substrate along a straight line ($y = 0$, $z = h$) at a constant velocity, u_b. The start point of the scanning is $x = -(l - r_0)$ and the end point is $x = (l - r_0)$, and therefore the total distance that the laser beam travels is $2(l - r_0)$.

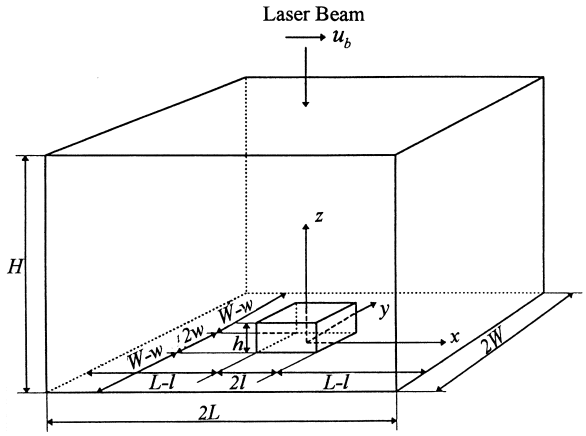

Fig. 1. Physical model of selective area laser deposition (SALD).

The vapor deposition starts after the surface temperature reaches the chemical reaction temperature. The chemical reaction that takes place on the top substrate surface absorbs part of the laser energy and consumes the $TiCl_4$ near the substrate surface. A concentration difference is therefore established and becomes the driving force of mass transfer. The laser energy absorbed by the substrate surface will be divided into three parts after the chemical reaction starts: the first part goes into the substrate through conduction, the second part is absorbed by the chemical reaction, and the third part is transferred into the gas through conduction since natural convection is neglected. Therefore, the physical model of the SALD process will include three parts: heat transfer in the substrate and gases, chemical reaction, and mass transfer in the gases.

2.1. Heat transfer

Since the temperature of the substrate undergoes a significant change under laser irradiation, the constant thermal properties assumption does not apply [5,9,10]. Since natural convection in the gases is negligible [10], heat transfer in the substrate and gases is modeled as one conduction problem with thermal properties reflecting the differences in each region. The advantage of modeling the conduction problem in the substrate and the gases as one problem is that the temperature distribution in substrate and gases can be obtained by solving one equation, and the iteration procedure to match the boundary condition at substrate–gases interface can therefore be eliminated. Since the problem is symmetric about the xz-plane, only half of the problem need to be investigated. For a coordinate system shown in Fig. 1, the heat conduction in the substrate and gases is governed by the following equation:

$$\frac{\partial(\rho c_p T)}{\partial t} = \frac{\partial}{\partial x}\left(k\frac{\partial T}{\partial x}\right) + \frac{\partial}{\partial y}\left(k\frac{\partial T}{\partial y}\right) + \frac{\partial}{\partial z}\left(k\frac{\partial T}{\partial z}\right) + S \tag{2}$$

where the thermal properties are different for substrate and gases.

$$k = \begin{cases} k_s & |x| \le l, \quad y \le w, \quad z \le h \\ k_g & |x| > l, \quad y > w, \quad z > h \end{cases} \tag{3}$$

$$\rho c_p = \begin{cases} (\rho c_p)_s & |x| \le l, \quad y \le w, \quad z \le h \\ (\rho c_p)_g & |x| \le l, \quad y \le w, \quad z \le h \end{cases} \tag{4}$$

The thermal properties of substrate material, Incoloy 800, can be obtained from Refs. [13,14]. The thermal conductivity and specific heat of the gases in the chamber is related to the individual thermal properties of H_2, N_2, and $TiCl_4$ as well as their molar fractions [15]. The thermal conductivities and specific heats of H_2 and N_2 at different temperature are obtained from Ref. [16]. Thermal conductivity and viscosity of $TiCl_4$ are derived by the method described in Ref. [15] because they are not available from the existing literature. The specific heat of $TiCl_4$ was obtained from JANAF Thermochemical Tables [17].

The source term in Eq. (2) deals with the effect of laser beam heating and chemical reaction since the interface between substrate and gases is located inside the system. The source term will be zero everywhere except at the substrate-gases interface under the laser spot. The heat flux at the substrate surface due to laser beam irradiation and chemical reaction is expressed as

$$q'' = \frac{2P\alpha_a}{\pi r_0^2}\exp\left[-\frac{(x - x_{st} - ut)^2 + y^2}{r_0^2}\right] - \epsilon\sigma\left(T^4 - T_\infty^4\right) - \rho_{TiN}\Delta H_R \frac{d\delta}{dt}, \; z = h \tag{5}$$

where $\frac{d\delta}{dt}$ is the deposit rate. The values of $\frac{d\delta}{dt}$ need to be determined by the chemical model that will be presented later. In order to use Eq. (5) to determine the source term in Eq. (2), the heat flux is treated as an internal heat source in the grid near the surface of the substrate, i.e.

$$S = \frac{q''\Delta x \Delta y}{\Delta V} = \frac{q''}{\Delta z} \tag{6}$$

where, Δx, Δy, Δz represent the dimension of the control volume cell in the substrate near its surface.

The initial and boundary conditions of the problem are

$$T = T_i, \quad -L \le x \le L, \quad 0 \le y \le W, \quad 0 \le z \le h, \quad t = 0 \tag{7}$$

$$\frac{\partial T}{\partial x} = 0, \qquad x = \pm L \tag{8}$$

$$\frac{\partial T}{\partial y}, \qquad y = 0, W \tag{9}$$

$$\frac{\partial T}{\partial z}, \qquad x = 0, H \tag{10}$$

From Eqs. (8)–(10), it is assumed that the heat loss to the outside of the chamber is negligible.

2.2. Chemical reaction

In the chemical reaction undergone in the vapor deposition of titanium nitride films, TiN is produced according to the overall chemical reaction expressed in Eq. (1) [7]. The production rate of TiN, which is defined as the mass of TiN produced per unit area per unit time, is calculated by

$$\dot{m} = K(T) C_{H_2} C_{N_2}^{1/2} C_{TiCl_4} \tag{11}$$

where $K(T)$ is the reaction rate constant and can be calculated by Arrhenius equation

$$K(T) = K_0' \exp\left(-\frac{E}{R_u T_s}\right) \tag{12a}$$

where T_s represent the upper surface temperature of the substrate.

Since the order of the magnitude of C_{H_2} and C_{N_2} is higher than that of C_{TiCl_4} for at least one order, the variation of C_{H_2} and C_{N_2} in the vapor deposition process can be neglected, i.e., C_{H_2} and C_{N_2} can be treated as constants in Eq. (11). Thus, one can define

$$K_0 = \left(C_{H_2}\right)_i \left(C_{N_2}\right)_i^{1/2} K_0' \tag{12b}$$

and Eq. (11) is rewritten as

$$\dot{m} = K_0 \exp\left(-\frac{E}{R_u T_s}\right) C_{TiCl_4} \tag{13}$$

The deposit rate is then expressed as

$$\frac{d\delta}{dt} = \frac{\dot{m}}{\rho_{TiN}} = \frac{K_0}{\rho_{TiN}} \exp\left(-\frac{E}{R_u T_s}\right) C_s \tag{14}$$

where the subscript of C_{TiCl_4} is dropped for notation and C_s in Eq. (14) represents the concentration of $TiCl_4$ at the surface of the substrate.

2.3. Mass transfer

Since variation of the concentration of N_2 and H_2 in the vapor deposition process is neglected, and therefore the concentration of N_2 and H_2 is assumed to be uniformly equal to their initial values. From Eq. (14), it can be seen that the deposition rate depends on the concentration of $TiCl_4$ at the top surface of substrate. Therefore, the concentration of $TiCl_4$ must be solved in order to predict the deposition rate. In the absence of natural convection in the chamber, the concentration of $TiCl_4$ is governed by the following mass diffusion equation

$$\frac{\partial C}{\partial t} = D\left(\frac{\partial^2 C}{\partial x^2} + \frac{\partial^2 C}{\partial y^2} + \frac{\partial^2 C}{\partial z^2}\right) + S_c \tag{15}$$

The mass diffusivity of $TiCl_4$ in the gas mixture is determined by Stefan–Maxwell equation [15] using the binary diffusivity of $TiCl_4$ with respect to each other species, which was calculated using the hard sphere model [15].

In order to have the same computational domain as the heat transfer problem, Eq. (15) applies to the entire computational domain, which includes substrate and gases. The concentration in the substrate area should satisfy $C \equiv 0$.The initial and boundary conditions of Eq. (15) are

$$C = C_i, \quad -L \le x \le L, \quad 0 \le y \le W, \quad 0 \le z \le h, \quad t = 0 \tag{16}$$

$$\frac{\partial C}{\partial X} = 0, \qquad x = \pm L \tag{17}$$

$$\frac{\partial C}{\partial y} = 0, \qquad y = 0, W \tag{18}$$

$$\frac{\partial C}{\partial z} = 0, \qquad z = H \tag{19}$$

$$\frac{\partial C}{\partial z} = 0, \quad z = 0, \quad |x| > l, \quad y > w \tag{20}$$

$$C = 0, \quad z = 0, \quad |x| \le l, \quad y \le w \tag{21}$$

As in the heat transfer problem, the effect of the chemical reaction on the mass transfer is taken care by a source term in Eq. (15). The mass flux rate of $TiCl_4$ at the substrate is expressed as

$$\dot{m}_{TiCl_4} = \rho_{TiN}\frac{d\delta}{dt}\frac{M_{TiCl_4}}{M_{TiN}}, \quad z = h \tag{22}$$

The source term in Eq. (15) is then expressed as

$$S_c = -\frac{\dot{m}_{TiCl_4}\Delta x \Delta y}{\Delta V} = -\frac{M_{TiCl_4}}{M_{TiN}}\frac{K_0}{\Delta z} \times \exp\left(-\frac{E}{R_u T_s}\right) C_s, \quad z = h \tag{23}$$

3. Numerical solution

Eqs. (2) and (15) are typical diffusion equations which can be discretized by a finite volume method [18] and solved numerically. The solution of the chemical reaction model is straightforward because the deposit rate is a explicit function of the temperature and concentration at the substrate surface. The iteration for a time step is outlined as follows:

1. Guess a distribution of deposit rate, $\frac{d\delta}{dt}$.
2. Solve for the temperature distribution in substrate and gases.
3. Solve for the concentration distribution in the gases.
4. Calculate the deposit rate, $(\frac{d\delta}{dt})_{new}$ from Eq. (14).
5. Compare the deposit rate obtained in step 4 with the guessed distribution in step 1. If $|(\frac{d\delta}{dt})_{new} - \frac{d\delta}{dt}|_{max} \le e$, where e is a small tolerance value, end the iteration and go to the next time step. If not, update the value of $\frac{d\delta}{dt}$ and go back to step 1.

During the above iteration procedure, an underrelaxation with underrelaxation factor of 0.5 is necessary. The calculations were carried out for a non-uniform grid of 112 nodes in the x-direction and 42 nodes in the y- and z-directions. The time step is 0.1 s for the cases of stationary laser and $\Delta t = 0.02$–0.05 s, which depends on the scanning velocity, for the cases of moving laser beam. Finer grid sizes ($162 \times 62 \times 62$) and smaller time steps (0.01 s) were also used in the calculations, but the difference on chemical deposit rate is less than 1%.

4. Results and discussion

In order to compare the calculated results with the experimental data, the geometric and physical parameters are same as those in Refs. [7,8]. The size of the chamber is $2L \times 2W \times H = 0.5 \times 0.5 \times 0.125$ m^3, and the substrate is $2l \times 2w \times h = 0.01 \times 0.01 \times 0.005$ m^3. The total pressure in the chamber is assumed to be 207 torr and the partial pressure of titanium chloride is maintained at 7 torr. The partial pressures of N_2 and H_2 are approximately the same. The absorptivity of the laser beam at the substrate surface is taken to be 0.23 which is a relatively higher due to multiple refections of the laser beam in the microcavities formed by the microstructures grown during the SALD process [7]. The radius of the laser beam, which is defined as the radius where the laser intensity is $1/e^2$ of the intensity at the center of the laser beam, is 1.0×10^{-3} m. The activation energy of the chemical reaction is taken to be $E = 51.02$ kJ/mol. The constant K_0, as defined in Eq. (12b), is 8.4 m/s. Chemical reaction heat, ΔH_R, as determined using JANAF thermochemical tables [17], is 5.379×10^6 J/kg. Volcano-like profiles of deposited film were often reported for the laser vapor deposition process [9] and the causes were not clear. Conde et al. [7] suggested that the low sticking coefficient at the center of the laser beam, where the

temperature is highest, plays a major role. A sticking coefficient, γ_{TiN}, introduced by Conde et al. [7] is employed in this paper to predict volcano-like deposited film.

The SALD process with a stationary laser beam is investigated first and the results are compared with the experimental data. Fig. 2(a) shows the variation of deposited TiN film thickness with different x but $y = 0$. Both predicted and experimental [7] results are plotted in Fig. 2(a). The power of the laser beam and

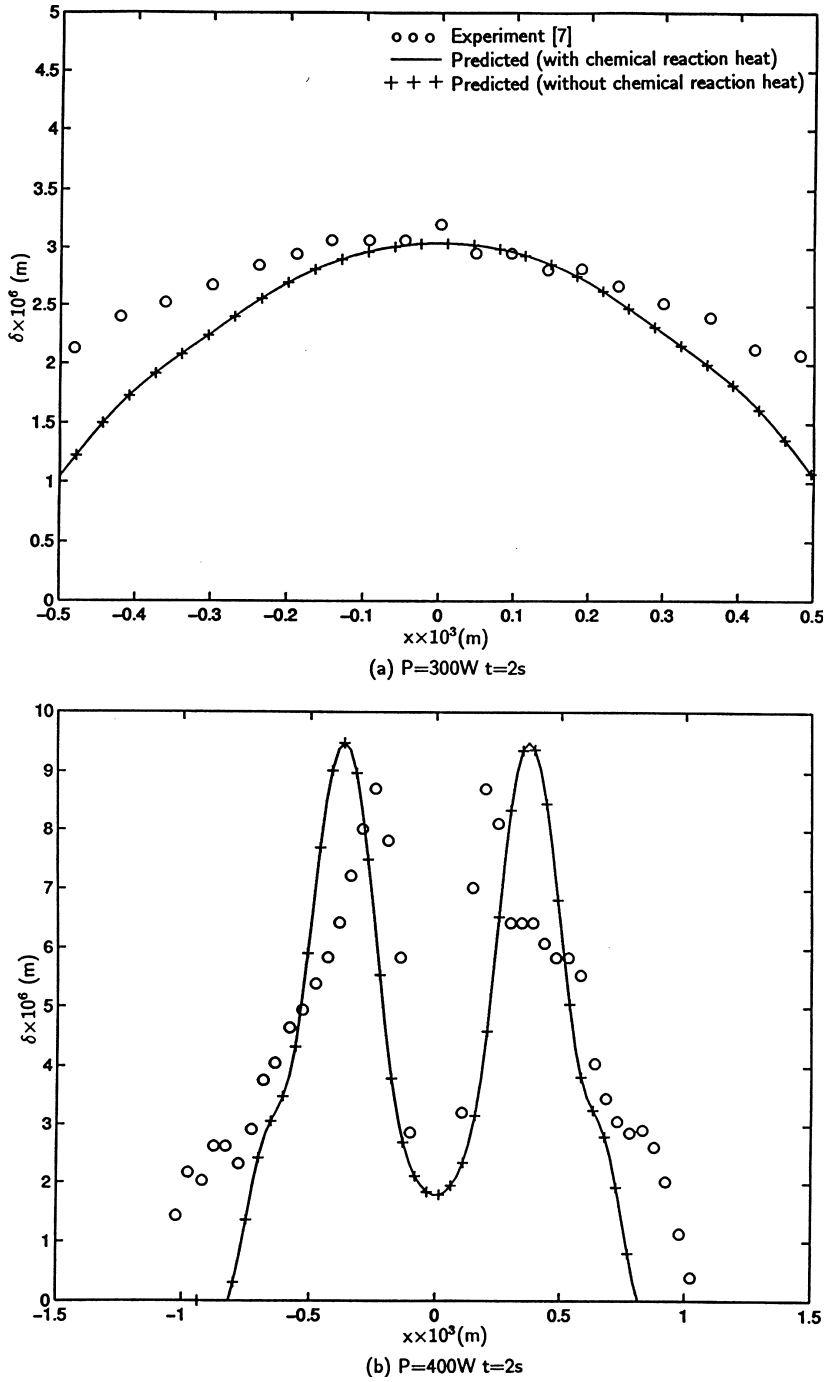

Fig. 2. Comparison of deposited TiN film profile obtained by numerical solution and experiment.

the irradiate time are 300 W and 2 s. It can be seen that the agreement between the predicted and experimental results is very good, especially at the center of the laser beam. The agreement between predicted and experimental results becomes poor at the locations that are far from the center of the laser beam. Fig. 2(b) shows the comparison of predicted deposited TiN film thickness with the experimental data in Ref. [7]. It can be seen that the quality agreement between the predicted result and the experimental data is very good. The volcano-like deposited film shape is successfully predicted by using the temperature dependence of the sticking coefficient introduced by Conde et al. [7]. Also plotted in Fig. 2(a) and (b) are the shapes of the deposited film in absence of chemical reaction heat, i.e., $\Delta H_R = 0$ in Eq. (5). It can be seen that the effect of chemical reaction heat on the shapes of deposited film is negligible because the effect of chemical reaction heat on the heat flux at the substrate surface is very insignificant. For the results shown in Fig. 2(a) and (b), the fraction of laser energy absorbed by the chemical reaction is less than 0.1%.

The SALD with moving laser beam is then investigated because it is the case for the real SALD process. Fig. 3 shows the 3D shape of the deposited film with laser power of 300 W and constant scanning velocity of 1 mm/s. It can be seen that both the height and width of the deposited film increase with increase of x. This occurs because the top surface temperature of the substrate at the center of the laser beam is lower when the scanning process is just started and increases with increases of the scanning time.

The temperature contours at $y = 0$ surface for the case of stationary laser beam and moving laser beam are shown in Fig. 4(a) and (b), respectively. For both cases, the region in the substrate and gases affected by the laser beam is very small. The chemical reaction is limited in the region where the surface temperature is higher than the threshold temperature (1173 K). Therefore, the TiN film can be deposited on the selected area by laser chemical vapor deposition, which is impossible for the conventional chemical vapor deposition process. For the case with moving laser beam, the affected zone to the negative direction of x-axis is larger than that to the positive direction of x-axis because the laser beam moves toward the positive direction of the x-axis. However, this difference is not significant for the isothermal lines at high temperatures because the moving velocity of the laser beam is actually very slow.

Fig. 5 shows the 3D shape of the deposited film with same laser power but slower scanning velocity of 0.8 mm/s. It can be seen that the deposited film is higher and wider than that at fast scanning velocity because the time the laser beam stays at a particular point is longer for a slower scanning velocity. In order to clearly see the effect of scanning velocity on the shape of the deposited film, the cross sections of the depos-

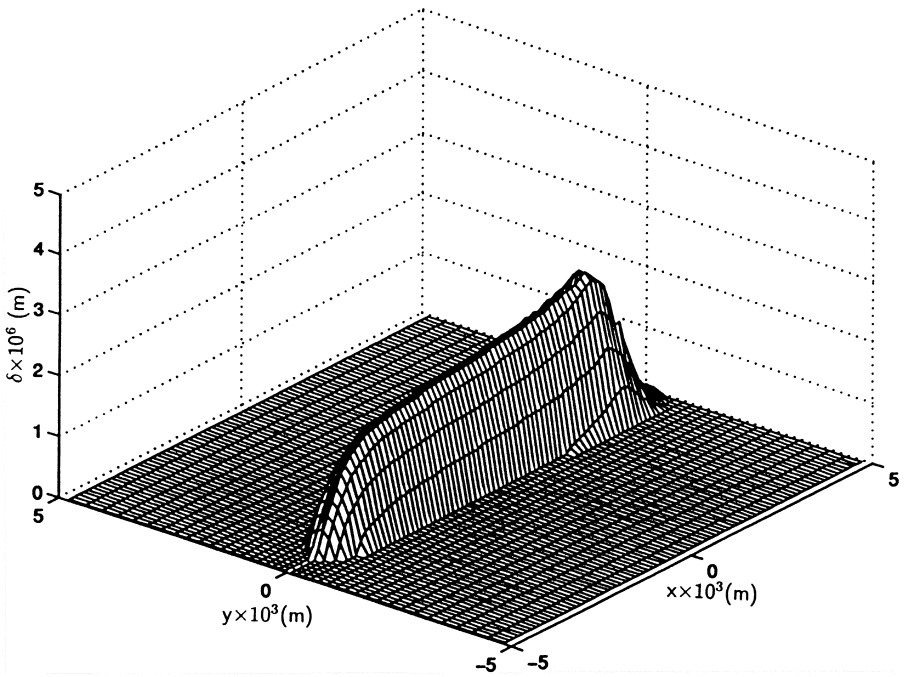

Fig. 3. 3D shape of the deposited TiN film with moving laser beam ($P = 300$ W $u = 1.0 \times 10^{-3}$ m/s and $t = 8$ s).

ited film at $y = 0$ and $x = 0$ for different scanning velocities are shown in Fig. 6.

Fig. 7 shows the shape of the deposited film for higher laser powers. The scanning velocity is same as in the case of Fig. 3, but the laser power is increased to 360 W. One thing that can be observed is that the deposited film is much higher and wider than that at a lower power of 300 W. The other thing that can be observed is that there is a x-direction groove on the top of the deposited film because the larger laser

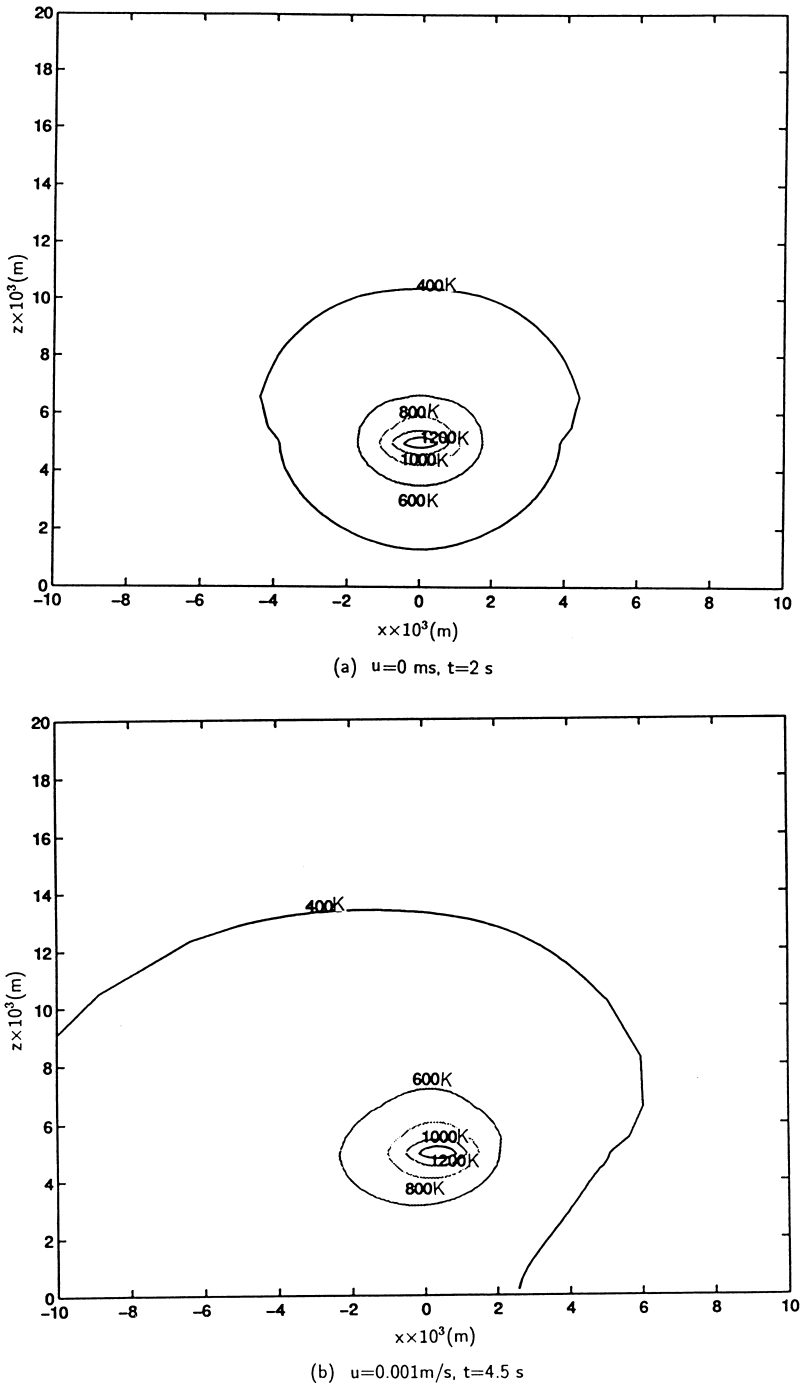

Fig. 4. Temperature contour at $y = 0$ ($P = 300$ W).

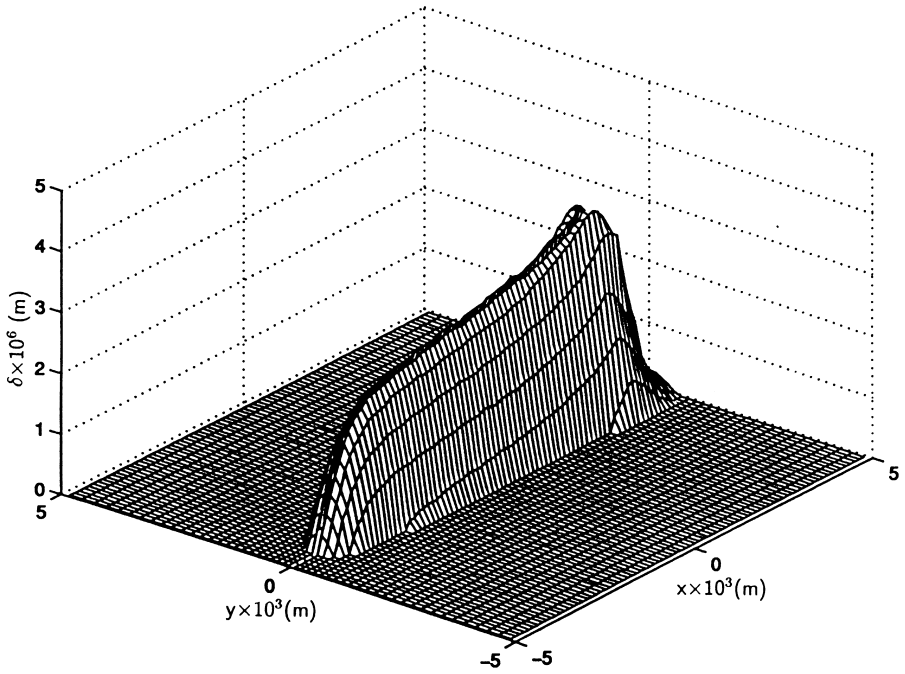

Fig. 5. 3D shape of the deposited TiN film with moving laser beam ($P = 300$ W $u = 0.8 \times 10^{-3}$ m/s and $t = 10$ s).

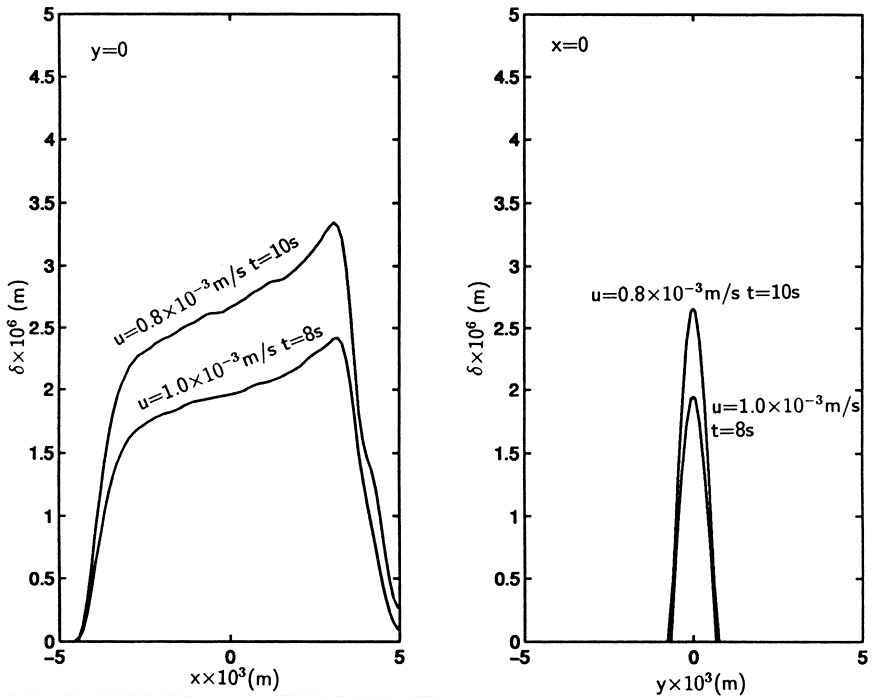

Fig. 6. Effect of scanning velocity on the cross section of the deposited film ($P = 300$ W).

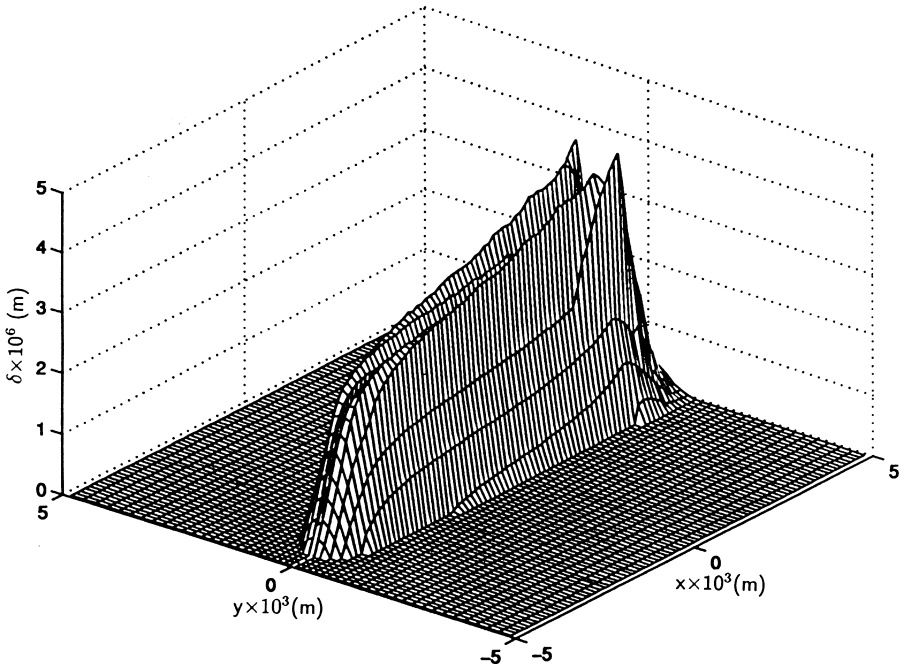

Fig. 7. 3D shape of the deposited TiN film with moving laser beam ($P = 360$ W, $u = 1.0 \times 10^{-3}$ m/s and $t = 8$ s).

power makes the top surface temperature of the substrate in some points exceed the critical temperature, above which the product of the chemical reaction can not be fully stuck on the substrate surface. In lieu of formation of the volcano-like film in the case of stationary laser beam, a groove is formed on the top of the deposited film. The groove on the top of the deposited film can be avoided by increasing scanning

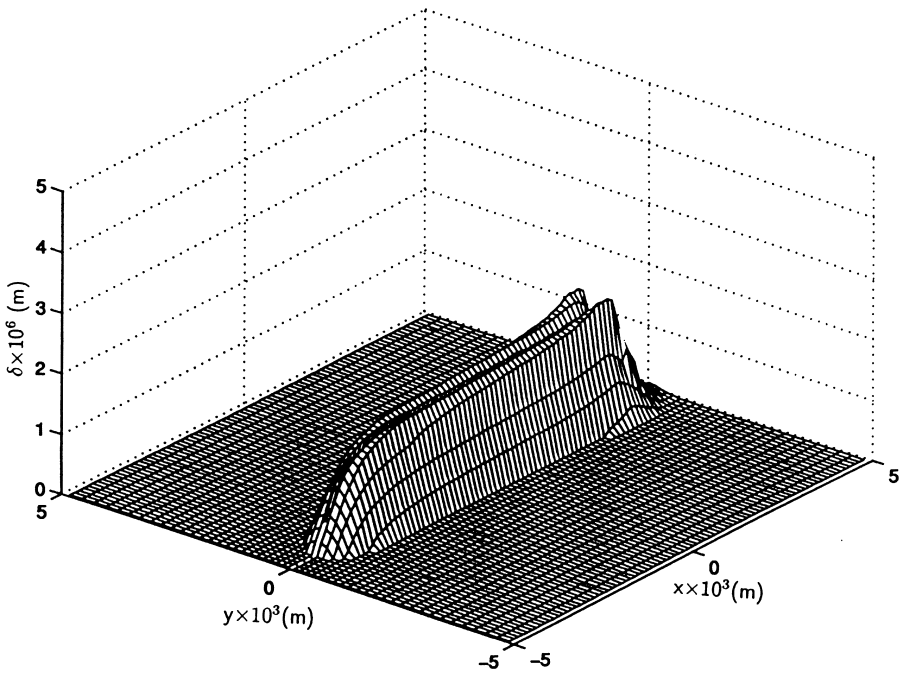

Fig. 8. 3D shape of the deposited TiN film with moving laser beam ($P = 360$ W, $u = 1.6 \times 10^{-3}$ m/s and $t = 5$ s).

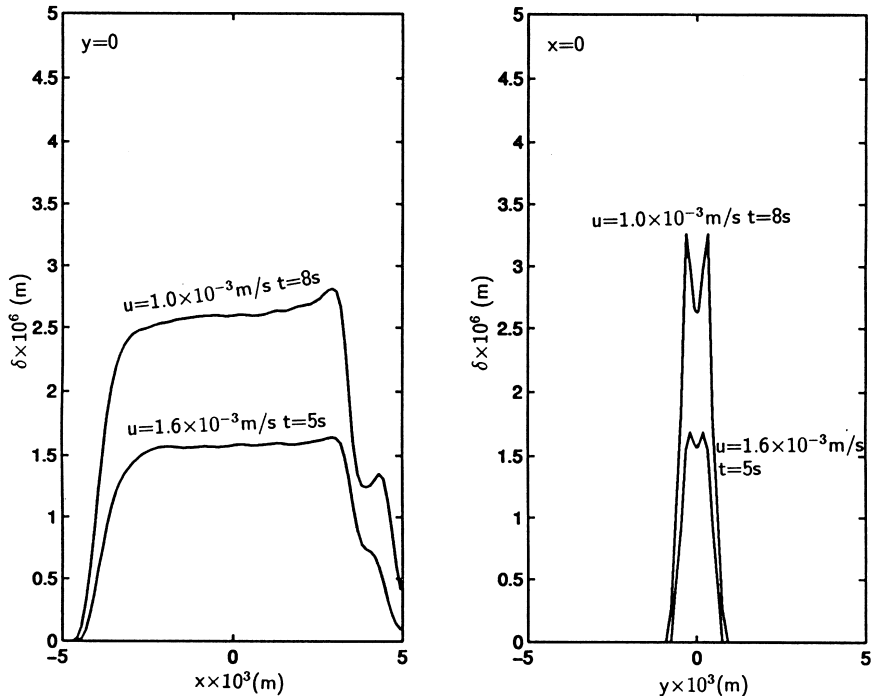

Fig. 9. Effect of scanning velocity on the cross section of the deposited film (P = 360 W).

velocity of the laser beam so that the top surface temperature of the substrate under the laser spot can be reduced. The 3D deposited film at the increased scanning velocity is shown in Fig. 8. It can be seen that the deposited film is thinner and more narrow and the groove on the top of the deposited film becomes very shallow. The effect of the scanning velocity on the cross section of the deposited film at $y = 0$ and $x = 0$ is shown in Fig. 9.

5. Conclusion

A thermal model of SALD process, which includes the submodels of heat transfer, chemical reaction and mass transfer, has been developed and the model is employed to simulate the laser vapor deposition of TiN film. The results show that the effect of chemical reaction heat on the shape of deposited film is negligible. For the cases with a stationary laser beam, the qualitive agreement between the predicted and experimental results are very good. The cases with moving laser beam are also investigated. The deposited film becomes higher and wider when the scanning velocity is decreased or the laser power is increased. The deposited film with a groove on the top is obtained for cases of higher laser power due to low the sticking coefficient of TiN at high temperatures.

References

[1] J.G. Conley, H.L. Marcus, Rapid prototyping and solid freeform fabrication, J. of Manufacturing Science and Engineering 119 (1997) 811–816.
[2] H.L. Marcus, G. Zong, P.K. Subramanian, Residual stresses in laser processed solid freeform fabrication, in: E.V. Barrera, I. Dutta (Eds.), Residual Stresses in Composites: Measurement, Modeling and Effect on Thermomechanical Properties, TMS, 1993.
[3] R.L. Marhajan, Transport phenomena in chemical vapor-deposition systems, in: Advances in Heat Transfer, Academic Press, San Diego, 1996.
[4] J. Mazumder, A. Kar, Theory and Application of Laser Chemical Vapor Deposition, Plenum Press, New York, 1995.
[5] A. Kar, J. Mazumder, Three-dimensional transient thermal analysis for laser chemical vapor deposition on uniformly moving finite slabs, J. of Applied Physics 65 (1989) 2923–2934.
[6] A. Kar, M.N. Azer, J. Mazumder, Three-dimensional transient mass transfer model for laser chemical vapor deposition of titanium on stationary finite slabs, J. of Applied Physics 69 (1991) 757–766.
[7] O. Conde, A. Kar, J. Mazumder, Laser chemical vapor

deposition of TiN dot: a comparison of theoretical and experimental results, J. Applied Physics 72 (1992) 754–761.

[8] O. Conde, M.L.G. Ferreira, P. Hochholdinger, A.J. Silvestre, CO_2 laser induced CVD of TiN, Applied Surface Science 54 (1992) 130–134.

[9] Y. Jacquot, G.-S. Zong, H.L. Marcus, Modeling of selective laser deposition for solid freeform fabrication, in: Proceedings of Solid Freeform Fabrication Symposium, 1995, pp. 74–82.

[10] Y.L. Lee, J.V. Tompkins, J.M. Sanchez, H.L. Marcus, Deposition rate of silicon carbide by selected area laser deposition, in: Proceedings of Solid Freeform Fabrication Symposium, 1995, pp. 433–439.

[11] Y. Zhang, Thermal modeling of advanced manufacturing technologies: grinding, laser drilling, and solid freeform fabrication, Ph.D. Dissertation, University of Connecticut, Storrs, CT, 1998.

[12] K.E. Torrance, Natural convection in thermally stratified enclosure with localized heating from below, J. of Fluid Mechanics 95 (3) (1979) 477–495.

[13] J.R. Davis, Heat-resistant materials, in: ASM Specialty Handbook, ASM International, Materials Park, OH, 1997.

[14] Y.S. Touloukian, Thermophysical Properties of High Temperature Solid Materials, vol. 3: Ferrous Alloys, Thermophysical Properties Research Center, Purdue University, West Lafayette, IN, 1967.

[15] R.B. Bird, W.E. Stewart, E.N. Lightfoot, Transport Phenomena, Wiley, New York, 1960.

[16] F.P. Incropera, D.P. DeWitt, Fundamentals of Heat and Mass Transfer, 4th ed., Wiley, New York, 1996.

[17] W.M. Chase, JANAF thermochemical tables, 3rd ed., J. Phys. Chem. Ref. Data 14 (1) (1986).

[18] S.V. Patankar, Numerical Heat Transfer and Fluid Flow, Hemisphere, Washington, DC, 1980.